Atmos. Chem. Phys. Discuss., 13, 1455–1488, 2013
www.atmos-chem-phys-discuss.net/13/1455/2013/
doi:10.5194/acpd-13-1455-2013

Atmospheric Chemistry and Physics Discussions

New particle formation in the western Yangtze River Delta: first data from SORPES-station

E. Herrmann[1,2], A. J. Ding[1], T. Petäjä[2], X. Q. Yang[1], J. N. Sun[1], X. M. Qi[1], H. Manninen[2], J. Hakala[2], T. Nieminen[2], P. P. Aalto[2], V.-M. Kerminen[2], M. Kulmala[2], and C. B. Fu[1]

[1]School of Atmospheric Sciences and Institute for Climate and Global Change Research, Nanjing University, Nanjing, China
[2]Department of Physics, University of Helsinki, Helsinki, Finland

Received: 19 December 2012 – Accepted: 3 January 2013 – Published: 15 January 2013

Correspondence to: E. Herrmann (eherrman@nju.edu.cn) and A. J. Ding (dingaj@nju.edu.cn)

Published by Copernicus Publications on behalf of the European Geosciences Union.

Abstract

Aerosols and new particle formation were studied in the western part of the Yangtze River Delta (YRD), at the SORPES station of Nanjing University. Air ions between 0.8 and 42 nm were measured using an air ion spectrometer; a DMPS provided particle size distributions between 6 and 800 nm. Additionally, meteorological data, trace gas concentrations, and $PM_{2.5}$ values were recorded. During the measurement period from 18 November 2011 to 31 March 2012, the mean total particle concentration was found to be 23 000 cm^{-3}. The mean $PM_{2.5}$ value was 90 $\mu g\,m^{-3}$, well above national limits. During the observations, 26 new particle formation events occurred, typically producing 6 nm particles at a rate of 1 $cm^{-3}\,s^{-1}$, resulting in over 4000 cm^{-3} new CCN per event. Typical growth rates were between 6 and 7 $nm\,h^{-1}$. Ion measurements showed the typical cluster band below 2 nm, with total ion concentrations roughly between 600 and 1000 cm^{-3}. A peculiar feature of the ion measurements were the heightened ion cluster concentrations during the nights before event days. The highly polluted air of the YRD provides both the potential source (SO_2) and the sink (particulate matter) for sulfuric acid, leaving radiation as the determining force behind new particle formation. Accordingly, a good correlation was found between new particle formation rate and radiation values.

1 Introduction

Atmospheric aerosols play a significant role in the Earth's radiative balance. They scatter and reflect incoming sunlight (direct effect; Twomey, 1974; Charlson et al., 1992; Bellouin et al., 2008), affect cloud properties (indirect effect; Twomey, 1984, 1991; Lohmann and Feichter, 2005), and can prevent cloud formation under certain conditions (semi-direct effect; Hansen et al., 1997; Allen and Sherwood, 2010). As an additional effect, the modification of the planet's radiative balance leads to the changes in the terrestrial carbon sink (Gu et al., 2002). The IPCC Report 2007 has identified

ACPD
13, 1455–1488, 2013

aerosols as the main uncertainty in our understanding of radiative forcing. Aerosols also affect human health and have been linked to asthma, lung cancer, and cardiovascular diseases among others (e.g. Pope and Dockery, 2006).

A central phenomenon related to atmospheric aerosols is new particle formation (atmospheric nucleation), i.e. the production of particulate matter from pre-existing vapors (secondary aerosols) (Kulmala et al., 2012). New particle formation has been observed all over the world under a wide variety of conditions (Kulmala et al., 2004; Kulmala and Kerminen, 2008) which suggests that different processes may be at work. While sulfuric acid has been identified as the key vapor involved (e.g. Sipilä et al., 2010), the roles of organic vapors, air ions, and clusters are under discussion; their influence may well vary with environmental conditions. In order to monitor and understand climate change, forcing and related feedbacks, also including the role of aerosols and aerosol processes such as nucleation, Hari et al. (2009) have suggested the establishment of a global network of measurement stations.

The Yangtze River Delta (YRD) stretches from Shanghai to Nanjing, is home to 100 million people and the largest conglomerate of adjacent megacities in the world. It is one of the motors of Chinese industrial development and a hotspot of human activity also on a global scale. Its meteorological conditions, rapid urbanization, and environmental challenges are representative for large portions of eastern and southern Asia and southern America.

At the western end of the delta, outside the city of Nanjing, the Station for Observing Regional Processes of the Earth System (SORPES) is set up to measure mainly YRD background air masses (as opposed to Nanjing urban air). The station is designated to evolve into a "flagship station" according to the Hari et al. (2009) proposition and currently houses various aerosol, trace gas, and meteorological measurements. In this article, we present the first measurements of new particle formation performed at SORPES. The measurement period spans from 18 November 2011 to 31 March 2012, forming the longest and most comprehensive data set on aerosols and related variables in the region to date.

ACPD
13, 1455–1488, 2013

2 Measurement station

2.1 Site and location

SORPES-NJU is located some 20 km east of downtown Nanjing in Eastern China. The exact coordinates are 32.12° N and 118.95° E. Nanjing has a humid subtropical climate with high relative humidity during the whole year. Haze occurs frequently. In the summer, temperatures can be well above 30 °C while temperatures somewhat below 0 °C are not uncommon during the winter months. The station is situated on a hill rising about 40 m above its surroundings, overlooking the new campus of Nanjing University which can be considered a suburban environment. With prevailing easterly winds throughout the year, the station mainly monitors YRD background air. The station currently measures aerosols, trace gases, fluxes, radiation, and meteorological data. A detailed account of the measurement station and its intents and purposes is presented in Ding et al. (2012a).

The site is located in a relatively rural environment with few local emission sources within 2–3 km. There is a large petro-industrial zone located about 5–10 km northwest of the site, but because of prevailing winds from the east (Ding et al., 2012a) and some small hills between this zone and the site, these air masses are rarely transported to the site. Besides these, an important local source of PM worthwhile to be mentioned is the wind-blow road dust. As there were intensive construction activities in the campus and 2–5 km in the east and transport of soil and stones often made the road very dirty and that dust can easily be blown by strong wind and vehicle-introduced turbulence, especially in the dry winter seasons. These activities generally caused a pollution of coarse mode particles. The mainly regional sources located in the East and Southeast direction with a distance up to 300 km, with many factories/power plants located along the Yangtze river and more developed cities, such as Shanghai, Suzhou, Wuxi, Changzhou and Nanjing city clusters, located in the South side of the Yangtze river.

ACPD
13, 1455–1488, 2013

2.2 Instrumentation and measurements

The central aerosol instrumentation used in this study consists of an air ion spectrometer (AIS) and a differential mobility particle sizer (DMPS, built at Helsinki University). Similar combinations have previously been successfully used in the study of atmospheric nucleation (e.g. Manninen et al., 2010).

The AIS consists of two parallel DMAs (differential mobility analyzer) for negative and positive air ions, respectively. The inner walls of the DMAs are outfitted with electrometers allowing for a direct detection of the currents caused by ion impact on the wall. The AIS detects ions between 0.8 and 42 nm (mobility) diameter in 21 channels (size ranges) per DMA. During the measurements presented here, the AIS was operated in a 2 plus 1 min cycle (2 min sampling plus 1 min background determination), making for a time resolution of 3 min. To minimize data deterioration caused by the deposition of particles on the inner surfaces of the DMAs, both analyzers had to be cleaned thoroughly at least once per month. Deposition of dirt onto the nets inside the venturi flow tubes can lower the flow rate and thus effect the operation of the mobility analyzers. Those nets were cleaned at least once per week. Poor quality data was excluded from further numerical analysis. The AIS in detail is described in Mirme et al. (2007).

The differential mobility particle sizer used in this study can be described as a "virtual twin" DMPS, i.e. a single DMPS run at two different flow rates to extend its size range (Salma et al., 2011). The inlet in equipped with an impactor of 2.5 µm cutoff diameter to avoid the deposition of large particles inside the instrument. The sample is dried using nafion tubes, and equilibrium charge is ensured by two americium 241 sources (each about 37 kBq). Particles are counted by a TSI 3772 butanol CPC (condensation particle counter). The DMPS provides the number size distribution between 6 and 800 nm mobility diameter. The time resolution is 10 min.

Besides aerosol and air ion size distribution data, this study also uses the following data: $PM_{2.5}$, global radiation, temperature, wind speed and direction, ozone

ACPD
13, 1455–1488, 2013

concentration, and SO_2 concentration. All instruments used are listed in Table 1 and more detailed descriptions of the instrumentations were given by Ding et al. (2012a).

3 Conditions during the measurement period

3.1 Meteorology

The data presented in this study covers the period from the middle of November 2011 to the end of March 2012, i.e. local winter, framed by late autumn and early spring. The average mean temperature during this period was 5.2 °C, with daily averages from −3.0 to 20.2 °C. The temperature profile (Fig. 2, upper left panel) is characterized by quite a regular oscillating shape indicating the passing of cold fronts. Throughout the measurement period, daily average temperatures have oscillated by as much as 10 °C within a few days. However, underlying this fluctuation, the seasonal trend is clearly visible.

The radiation plot in Fig. 2 does not exhibit a clear seasonal behavior for most of the measurement period as the change in the Sun's position would suggest. The significance of this observation will be discussed in the sections relating to nucleation frequency and nucleation characteristics. However, the radiation data plot quite convincingly conveys its anti-correlation with the humidity data in the same panel: high humidity suggests rain or clouds which again means less radiation at ground level. The wind direction histogram in the right panel reflects the dominance of easterly winds with the main wind direction being around 70° and almost all wind directions between 30° and 120°. This means that the station hardly ever sees pollution from downtown Nanjing in the west and the industrial zone in the northwest while air masses from the YRD occur frequently. The impact of this on aerosol characteristics and new particle formation will be discussed in the appropriate sections.

ACPD
13, 1455–1488, 2013

3.2 Aerosol characteristics

Figure 3 illustrates how air ion concentrations and particle mode concentration depend on wind direction. In the figure, ion clusters is the sum of positive and negative ions below 2 nm. The nucleation mode covers the range from 6 to 25 nm, the Aitken mode from 25 to 90 nm, and the accumulation mode from 90 to 800 nm.

Considering the ion clusters, the most interesting detail is the comparison to the accumulation mode panel. While the ion cluster concentration does not change much with wind direction, there seems to be a certain amount of anti-correlation with accumulation mode concentrations: those are the highest between 60° and 180°, while ion cluster concentrations are the lowest for the same wind directions. Especially suggestive is the ion cluster concentration bump between 330° and 360° which has a counterpart indentation in the accumulation mode concentration plot. However, this nice fit should not be overstated as winds from that direction are a rare occurrence (see Fig. 2) and statistics thus poor. In any case, the relationship between ion cluster and accumulation mode concentration can be easily enough explained with the coagulation sink which is caused by the accumulation mode particles and which is consuming small clusters and particles.

The nucleation mode panel has two main features. First, the average nucleation mode concentrations are relatively low in the prevailing wind direction (easterly). Second, when the wind comes from the north (0°–30°), nucleation mode concentrations are almost twice as high as for the other wind directions. These observations can be interpreted as a higher nucleation probability for northern air masses and a lower nucleation probability for other wind directions. Comparing this to the Aitken and especially the accumulation mode panel, we observe rather low concentrations in the Aitken and accumulation mode for northern air masses. This suggests that at least part of the higher nucleation mode concentrations (i.e. higher nucleation probability) in this sector can be explained as a consequence of lower concentrations of larger particles, i.e. a lower condensation sink. In accordance with this, quite large amounts of larger

ACPD
13, 1455–1488, 2013

particles are associated with easterly winds, explaining the lack of nucleation from this direction by the same mechanism.

During the measurement period from 18 November 2011 to 31 March 2012, on average (median), a total (sum of positive and negative ions) of 770 cm^{-3} ion clusters below 2 nm diameter were observed, with the 25 and 75 percentiles being 600 and 970, respectively, in line with earlier findings that the "cluster band" below 2 nm is ever-present and subject only to relatively small fluctuations (Hirsikko et al., 2005). Between 6 and 25 nm, i.e. in what could be considered the nucleation mode, a median of 3500 cm^{-3} particles was observed, with 25 and 75 percentiles of 2100 and 6000, respectively. For the Aitken mode (25–90 nm) and the accumulation mode (90–800 nm), the same figures are 8500, 6100, 11500, and 6600, 4700, 9100, respectively. To estimate the fraction of charged particles, we integrated ion and particle concentrations in the instruments' overlapping region from 6 to 30 nm. For the total particle to ion ratio we found a median value of 4.4 (percentiles 3.4 and 5.9). Table 2 lists these figures as well as means and 5 and 95 percentiles to characterize the aerosol population more completely. Of the modes, the nucleation and the Aitken mode naturally show the largest variations, accounting for days with and without new particle formation. The range in accumulation mode concentrations on the other hand, is not related to local phenomena but an indication of the pollution level of the incoming air masses. Accordingly, the median and percentiles for $PM_{2.5}$ (79, 47, 116 $\mu g\,m^{-3}$) quite closely follow the respective figures for the accumulation mode.

4 Nucleation event characteristics

New particle formation was observed on 26 days during the measurement period which makes for a nucleation probability of roughly 20 %. Nucleation occurred during all months of the measurements, with somewhat less activity during November and December (see Table 3). A pronounced "winter break" as seen in for example in Hyytiälä (Dal Maso et al., 2005, 2009) could not be observed. All recorded particle

ACPD
13, 1455–1488, 2013

formation events are of type Ib.2 (classification according to Hirsikko et al., 2007) with a noticeable gap between the cluster band (below 2 nm) and what is informally called the nucleation "banana". This (see Fig. 4) would indicate that particle formation has not started at the measurement site but was imported from a few kilometers off site. This is the case for all observed events, which suggests that particle formation directly at the site was suppressed by some mechanism during the measurement period. As mentioned above, the direct vicinity of the site is currently a construction ground. The dust released in these construction activities could act as a condensation sink for nucleating vapors and thus hinder particle formation. Alternatively, it is possible that nucleation occurs almost exclusively in the neutral realm, i.e. that ion-induced nucleation plays a very minor role. The first stages of new particle formation would then be invisible to our instrumentation. The first possibility can be addressed with long-term measurements that cover changing conditions at the site. To verify the role of ion-induced nucleation, however, the detection of neutral particles would have to be extended to sizes well below 6 nm.

The gap (Fig. 4) makes it impossible to determine a reliable estimate of the growth rate for the smallest (< 3 nm) of the newly formed particles. For particles between 3 and 7 nm, AIS measurements yield a median growth rate of 5.9 $\mathrm{nm\,h^{-1}}$ with 25 and 75-percentiles of 4.4 and 7.9 $\mathrm{nm\,h^{-1}}$, respectively. From 7 to 30 nm, the AIS growth rate has a median of 6.7 $\mathrm{nm\,h^{-1}}$ (percentiles 5.2 and 8.2). Based on DMPS data, the growth rate between 6 and 30 nm is 6.9 $\mathrm{nm\,h^{-1}}$ (percentiles 6.1 and 10.9) while larger particles grow almost as fast at 6.6 $\mathrm{nm\,h^{-1}}$. The observed formation rate (averaged over the whole event) of 6-nm-particles J_6 is 0.82 $\mathrm{cm^{-3}\,s^{-1}}$ (percentiles 0.51 and 1.23). Following the method outlined by Kulmala et al. (2012), the formation rate of 2-nm-particles J_2, i.e. the actual nucleation rate, was estimated at a median value of 23.9 $\mathrm{cm^{-3}\,s^{-1}}$ with percentiles 14.8 and 56.8, respectively. During one new particle formation event, a median number of 18 000 $\mathrm{cm^{-3}}$ 6-nm-particles is produced (percentiles 7300 and 29 000). And more significantly, 4400 $\mathrm{cm^{-3}}$ new cloud condensation nuclei (CCN) are formed (percentiles 2800 and 5400). During events, the condensational sink had a median

ACPD
13, 1455–1488, 2013

value of 0.025 s^{-1} (percentiles 0.02 and 0.03) while over the whole measurement period, the median CS was 0.04 (percentiles 0.03 and 0.055).

Figure 5 shows the median daily cycles for the concentrations of air ions below 2 nm (ion clusters), from 2–7 nm (intermediate ions), and from 7–20 nm (large ions). As Fig. 4 illustrates, under conditions of no new particle formation, there is a gap between the cluster band and the background aerosol population which starts roughly around 10 nm. This gap is populated only during new particle formation events. This is reflected in the daily curves for intermediate ions which, essentially, can be observed only during nucleation days. It also shows, albeit not as prominently, in the case of large ions whose event day concentrations rise significantly over the non-event case with some delay after nucleation can be seen in the intermediate ions. The delay in this case is the time the new particles need to grow into the large ion range.

An intriguing feature of Fig. 5 is the small, but as we believe significant difference in behavior of cluster ions (< 2 nm) for event and non-event days. The figure shows that cluster ions have heightened concentrations during event days before new particle formation sets in. It has to be noted that the peak in cluster ion concentration during event days occurs around 4 o'clock in the night, i.e. several hours before sunrise. The mechanism behind this behavior is unclear. A noteworthy detail is that the decline in cluster concentration (around 4 a.m.) coincides with a slight increase in intermediate ion concentration. While this increase is far too small to explain the cluster behavior, the same mechanism(s) might be at work. When new particle formation starts properly (i.e. between 9 and 10 a.m. as seen in the intermediate figure), the cluster concentration for event days has almost returned to the non-event level. Even though the data used in this analysis has been checked thoroughly and poor quality data has been removed generously, the small number of nucleation days and the small scale of the effect leave the possibility that the effect is not real. Further measurements are thus required to (i) verify these observations and (ii) gain some insight into its mechanisms.

ACPD
13, 1455–1488, 2013

5 Event conditions

5.1 Daily cycles

Sulfuric acid vapor has been identified as one of the key species in the first steps of new particle formation (e.g. Kulmala 2003). Since continuous measurements of atmospheric sulfuric acid vapor are relatively demanding and therefore quite frequently not available, a proxy has been developed to estimate the sulfuric acid concentration based on other data (Petäjä et al., 2009):

$$\text{Proxy} = k \cdot [SO_2] \cdot \text{glob\_rad}/\text{CS} \quad (1)$$

Here, $[SO_2]$ is the SO_2 concentration, glob_rad is global radiation, and CS the condensational sink for sulfuric acid which can be determined based on the aerosol size distribution (Dal Maso et al., 2002). The equation compares production of H_2SO_4 (for which radiation and SO_2 are central) to losses by deposition to existing aerosol particles (condensational sink). The factor k is a constant that describes local conditions; it differs with site and can only be determined by comparing to actual measurements of H_2SO_4. However, even if such measurements are not available, the proxy (without k) can provide valuable insight into the qualitative behavior of sulfuric acid.

Figure 6 presents daily cycles of the sulfuric acid proxy and its components for event and non-event days. The radiation panel shows an expected result: higher radiation values on event days. Radiation is needed to drive the atmospheric chemistry that eventually produces sulfuric acid. Comparing the SO_2 and condensation sink curves, one notices that their behavior is pretty similar, with generally lower levels on event days and especially the pronounced drop in CS (and $[SO_2]$) before noon, i.e. before new particle formation begins. While the CS behavior is typical for remote rural sites as well (Dal Maso, 2006), the strong correlation between CS and $[SO_2]$ is characteristic for polluted sites; CS and $[SO_2]$ both indicate polluted air. Since Eq. (1) has CS and $[SO_2]$ on different sides of the bar, both almost eliminate each other when calculating the sulfuric acid proxy. As a consequence, the proxy daily cycles strongly resemble

ACPD
13, 1455–1488, 2013

the radiation cycles. This means that under the polluted conditions at the site (and in the YRD), radiation values are possibly as good a sulfuric acid predictor as the proxy described above. Note that the CS panel also includes $PM_{2.5}$ data for comparison. Conceptually, both are somewhat similar, and since both $PM_{2.5}$ and an alternative proxy based on $PM_{2.5}$ behave very similarly to CS and the CS-based proxy, respectively, $PM_{2.5}$ data can be a valid alternative when CS data is not available.

5.2 Nucleation rate dependence and nucleation parameter

Figure 7 further studies which variables best correlate with new particle formation. To do so, we have plotted the observed formation rate J_6 against a number of parameters. In panel (a), this parameter is the proxy described above, in panel (b) the ratio of radiation and condensation sink, and, finally, in panel (c) simply the radiation. While panels (a) and (b) don't reveal any particularly strong correlations, the relation between radiation and J_6 in panel (c) is rather clearly visible. An exponential fit yields an R^2 of 0.46 which is quite high and further supports the above findings that radiation is the main determining factor behind new particle formation at the measurement site and probably under polluted conditions in general.

Based on the results of McMurry et al. (2005) a parameter was tested to separate event from non-event days. Using the sulfuric acid proxy, McMurry's nucleation criterion can be simplified and approximated by a parameter L' of the form

$$L' \sim \mathrm{CS}^2/([\mathrm{SO}_2] \cdot \mathrm{glob\_rad} \cdot \sqrt{T}) \quad (2)$$

where T is the temperature. As we have argumented above, CS and the SO_2 concentration behave very similarly, leading to an even more simplified L'':

$$L'' \sim \mathrm{CS}/(\mathrm{glob\_rad} \cdot \sqrt{T}) \quad (3)$$

The original parameter L was developed for the sulfur-rich conditions in Atlanta, and it is a fair assumption that the YRD does not suffer from any lack of sulfur in its atmosphere.

ACPD
13, 1455–1488, 2013

As Fig. 8 illustrates, the simplified L'' parameter manages to separate events and non-events to a certain extent, also clearly separating the respective quartiles. However, some overlap remains. Of course, this approach contains significant uncertainties, most noticeably the fact that the sulfuric acid proxy has not been verified against actual measurements. Thus the search for a working nucleation criterion clearly shows the importance of sulfuric acid measurements. Interestingly, the parameter in Fig. 8 appears to work somewhat better starting around mid-January. A full annual cycle of measurements will provide more insight into this observation and into the capabilities of the nucleation criterion and alternatives to improve it.

5.3 Role of incoming air masses

Wind direction and the origin and history of the incoming air masses have been found to play a significant role in new particle formation (Sogacheva et al., 2005; Dal Maso et al., 2007). Figure 9 summarizes the situation at the SORPES site for the measurement period. Panel (b) is a plot of the nucleation probability as a function of wind direction. This probability is quite high (around and over 40 %) for most wind directions, while being rather low for easterly winds (ca. between 45° and 100°). Incidentally, the direction of low nucleation probability is also the prevailing wind direction (compare to Fig. 2), amounting to a total nucleation probability of below 20 % as noted earlier.

To gain more insight into the relation of incoming air masses and nucleation behavior, we used the Hybrid Single-Particle Lagrangian Integrated Trajectory (HYSPLIT) dispersion model (Draxler and Hess, 1998) following a method described by Ding et al. (2012b). For each day when nucleation was observed, the model was run 1-day backwardly with 3000 particles released 100 m over the measurement site. Thus, a footprint retroplume was identified providing information about the origin and history of the observed air masses.

Panel (a) of Fig. 9 shows the 1-day retroplumes for the event days recorded during the measurement period. It is noteworthy that events were only observed when air masses were originating from the NNE half of the map (300°–120° in terms of wind

ACPD
13, 1455–1488, 2013

directions). It seems plausible that air masses from SSW typically pass over heavily polluted Nanjing and adjacent industrial areas and are therefore so saturated with particles that the high condensation sink makes new particle formation unlikely. The accumulation mode panel in Fig. 3 with the highest concentrations in the south supports this. Also the fact that wind from the SSW half is a rare occurrence (see Fig. 2) implies that nucleation contributions from the area are even more unlikely.

A striking feature of panel (a) is the "gap" to the east (ca. 100°–130°). This gap is home to Shanghai, Suzhou, and Wuxi – essentially all major cities in the YRD. Ding et al. (2012a) found an important potential source contribution from the city-cluster to trace gases and aerosol mass concentrations measured at the SORPES site. Figure 9a thus states that no new particle formation was observed with air masses coming from the cities of the YRD; high particle load seems again the most plausible explanation. The numbers in Table 5 further stress the point. Between 10 and 100 nm (i.e. where new particles should contribute), Gao et al. (2009) observed over 28 000 cm^{-3} particles at a site outside Shanghai, while we saw only 13 000 outside Nanjing. Part of the differences might well be explained with the measurement period, but the next column supports the theory that high pre-existing particle loads suppress nucleation: Between 100 and 500 nm, we observed almost fourfold particle concentrations at the Nanjing site. Considering prevailing easterly winds (i.e. from Shanghai and YRD), it is also fairly obvious that much of the accumulation mode observed at the SORPES site has its origin in the YRD.

6 Conclusions

The Station for Observing Regional Processes of the Earth System at Nanjing University (SORPES-NJU) is set up to measure atmospheric processes (a) continuously and (b) on a long-term basis. As part of the stations operations, aerosol and air ion measurements started in the end of 2011. The first results are presented in this paper.

ACPD
13, 1455–1488, 2013

From the middle of November 2011 to the end of March 2012, an air ion spectrometer (AIS) and a differential mobility particle sizer (DMPS) monitored the air ion (0.8–42 nm) and aerosol (6–800 nm) populations at a site outside Nanjing in the Yangtze River Delta in eastern China. For the total particle concentration N, the measured mean value of 2.3×10^4 cm^{-3} is of the same order of magnitude as similar observations in China, Europe, and the US (see Table 5). Interestingly, a much larger fraction of the total particle number is contributed by larger particles when comparing Nanjing to other (urban) locations, resulting in high $PM_{2.5}$ loads with a mean value of 90 µg m^{-3}, well above the annual national limit of 35 µg m^{-3} and even above the daily average limit of 75 µg m^{-3}. Observations give reason to assume that high accumulation mode concentrations are mainly imported from pollution sources east of Nanjing, i.e. from the YRD. Accordingly, not a single particle formation event was observed when air masses came in from the YRD.

New particle formation was observed on 26 days, making for a nucleation probability of almost 20 %. Typical growth rates for newly formed particles were between 6 and 7 nm h^{-1}, which falls well within the range observed for example in Europe (i.e. Manninen et al., 2010). An average nucleation day produced more than 4000 cm^{-3} new particles in the accumulation mode which can be considered new CCN. A peculiar feature of new particle formation at the site is a heightened ion cluster concentration during the night prior to nucleation onset. The mechanism behind this observation is unclear. A typical feature of nucleation events observed at the SORPES site is a gap between the cluster ion band and aerosol ions. This suggests that ion-induced nucleation is very insignificant or that particle formation is locally subdued, probably by pollution from the surrounding construction ground.

A comparison of conditions during nucleation event and non-event days showed that radiation is by far the most decisive factor while pollution variables $PM_{2.5}$ (or condensation sink) and SO_2 concentration more or less neutralize each other. Between the observed nucleation rate J_6 and global radiation, a quite strong correlation was found. McMurry's nucleation criterion (McMurry et al., 2005) was applied to the observations,

ACPD
13, 1455–1488, 2013

however, the parameter did not manage to perfectly separate event from non-event conditions.

While the data presented here are the most comprehensive study on aerosols and nucleation in the Yangtze River Delta and while they illustrate the power of integrated atmospheric measurements, they also stress the need for more observations. Annual and seasonal cycles need to be established, with respect to aerosols in general as well as to nucleation and its conditions to quantify the behavior of the aerosol population at the site. Also the effect of local conditions (ongoing construction) on aerosol measurements has to be evaluated. The pre-nucleation behavior of ion clusters needs to be verified and further analyzed. With year-round data it should also be possible to better evaluate the current nucleation criterion by McMurry and subsequently improve on it. Newly available measurements will help to analyze aerosol chemical composition in the future. An extension of the neutral detection range towards smaller sizer would make it possible to evaluate the role of ion-induced nucleation.

Acknowledgements. This work was funded by the 973 Program (2010CB428500), National Natural Science Foundation of China (No. 41275129/D0510), the Academy of Finland projects (1118615, 139656), and the European Commission via ERC Advanced Grant ATM-NUCLE. The SORPES-NJU stations were supported by the 985 program and the Fundamental Research Funds for Central Universities in China. We appreciate the contribution of Longfei Zheng, Yuning Xie, Longshan Jin, and Zhen Peng in the maintenance of the trace gases and meteorological instruments at the station.

References

Allen, R. J. and Sherwood, S. C.: Aerosol-cloud semi-direct effect and land-sea temperature contrast in a GCM, Geophys. Res. Lett., 37, L07702, doi:10.1029/2010GL042759, 2010.

Bellouin, N., Jones, A., Haywood, J., and Christopher, S. A.: Updated estimate of aerosol direct radiative forcing from satellite observations and comparison against the Hadley Centre climate model, J. Geophys. Res.-Atmos., 113, D10205, doi:10.1029/2007JD009385, 2008.

ACPD
13, 1455–1488, 2013

Charlson, R. J., Schwartz, S. E., Hales, J. M., Cess, R. D., Coakley Jr., J. A., Hansen, J. E., and Hoffman, D. J.: Climate forcing by anthropogenic aerosols, Science, 255, 423–430, doi:10.1126/science.255.5043.423, 1992.

Dal Maso, M., Kulmala, M., Lehtinen, K. E. J., Mäkelä, J. M., Aalto, P. P., and O'Dowd, C. D.: Condensation and coagulation sinks and formation of nucleation mode particles in coastal and boreal forest boundary layers, J. Geophys. Res.-Atmos., 107, 8097, doi:10.1029/2001JD001053, 2002.

Dal Maso, M., Kulmala, M., Riipinen, I., Wagner, R., Hussein, T., Aalto, P. P., and Lehtinen, K. E. J.: Formation and growth of fresh atmospheric aerosols: eight years of aerosol size distribution data from SMEAR II, Hyytiälä, Finland. Boreal Env. Res., 10, 323–336, 2005.

Dal Maso, M., Sogacheva, L., Aalto, P. P., Riipinen, I., Komppula, M., Tunved, P., Korhonen, L., Suur-Uski, V., Hirsikko, A., Kurtén, T., Kerminen, V.-M., Lihavainen, H., Viisanen, Y., Hansson, H.-C., and Kulmala, M.: Aerosol size distribution measurements at four Nordic field stations: identification, analysis and trajectory analysis of new particle formation bursts, Tellus B, 59, 350–361, doi:10.1111/j.1600-0889.2007.00267.x, 2007.

Dal Maso, M.: Analysis of atmospheric particle formation events, Ph. D. thesis, Helsinki, Finland, 2006.

Dal Maso, M., Hari, P., and Kulmala, M.: Spring recovery of photosynthesis and atmospheric particle formation, Boreal Environ. Res., 14, 711–721, 2009.

Ding, A. J., Fu C. B., Yang, X. Q., Sun, J. N., Zheng, L. F., Xie, Y. N., Herrmann E., Petäjä, T., and Kulmala, M.: Ozone and fine particle in the western Yangtze River Delta: an overview of 1-year data at the SORPES station, Atmos. Chem. Phys. Discuss., submitted, 2012a.

Ding, A . J., Wang, T., and Fu, C. B.: Transport characteristics and origins of carbon monoxide and ozone in South China: results from a Lagrangian dispersion simulation, J. Geophys. Res., in revision, 2012b.

Draxler, R. R. and Hess, G. D.: An overview of the HYSPLIT_4 modeling system for trajectories, dispersion, and deposition, Aust. Meteorol. Mag., 47, 295–308, 1998.

Gao, J., Wang, T., Zhou, X. H., Wu, W., and Wang, W. X.: Measurement of aerosol number size distributions in the Yangtze River Delta in China: formation and growth of particles under polluted conditions, Atmos. Environ., 43, 829–836, doi:10.1016/j.atmosenv.2008.10.046, 2009.

ACPD
13, 1455–1488, 2013

Gu L. H., Baldocchi D., Verma S. B., Black T. A., Vesala T., Falge E. M., and Dowty P. R.: Advantages of diffuse radiation for terrestrial ecosystem productivity, J. Geophys. Res.-Atmos., 107, 4050, doi:10.1029/2001JD001242, 2002.
Hansen J., Sato M., and Ruedy, R.: Radiative forcing and climate response, J. Geophys. Res., 102, 6831–6864, doi:10.1029/96JD03436, 1997.
Hari, P., Andreae, M. O., Kabat, P., and Kulmala, M.: A comprehensive network of measuring stations to monitor climate change, Boreal Environ. Res., 14, 442–446, 2009.
Hirsikko, A., Laakso, L., Hõrrak, U., Aalto, P. P., Kerminen, V.-M., and Kulmala, M.: Annual and size dependent variation of growth rates and ion concentrations in boreal forest, Boreal Environ. Res., 10, 357–369, 2005.
Hirsikko, A., Bergman, T., Laakso, L., Dal Maso, M., Riipinen, I., Hõrrak, U., and Kulmala, M.: Identification and classification of the formation of intermediate ions measured in boreal forest, Atmos. Chem. Phys., 7, 201–210, doi:10.5194/acp-7-201-2007, 2007.
IPCC 2007: Climate Change 2007: The Physical Science Basis – Contribution of Working Group I to the Fourth Assessment Report of the Intergovernmental Panel on Climate Change, edited by: Solomon, S., Qin, D., Manning, M., Chen, Z., Marquis, M., Averyt, K. B., Tignor, M., and Miller, H. L., Cambridge University Press, Cambridge, UK and New York, NY, USA, 2007.
Kulmala, M.: How particles nucleate and grow, Science, 302, 1000–1001, doi:10.1126/science.1090848, 2003.
Kulmala, M., Vehkamäki, H., Petäjä, T., Dal Maso, M., Lauri, A., Kerminen, V.-M., Birmili, W. and McMurry, P. H.: Formation and growth rates of ultrafine atmospheric particles: a review of observations, J. Aerosol Sci., 35, 143–176, doi:10.1016/j.jaerosci.2003.10.003, 2004.
Kulmala, M. and Kerminen, V.-M.: On the formation and growth of atmospheric nanoparticles, Atmos. Res., 90, 132–150, doi:10.1016/j.atmosres.2008.01.005, 2008.
Kulmala, M., Petäjä, T., Nieminen, T., Sipilä, M., Manninen, H. E., Lehtipalo, K., Dal Maso, M., Aalto, P. P., Junninen, H., Paasonen, P., Riipinen, I., Lehtinen, K. E. J., Laaksonen, A., and Kerminen, V.-M.: Measurement of the nucleation of atmospheric aerosol particles, Nat. Protoc., 7, 1651–1667, doi:10.1038/nprot.2012.091, 2012.
Lohmann, U. and Feichter, J.: Global indirect aerosol effects: a review, Atmos. Chem. Phys., 5, 715–737, doi:10.5194/acp-5-715-2005, 2005.
Manninen, H. E., Nieminen, T., Asmi, E., Gagné, S., Häkkinen, S., Lehtipalo, K., Aalto, P., Vana, M., Mirme, A., Mirme, S., Hõrrak, U., Plass-Dülmer, C., Stange, G., Kiss, G., Hoffer, A.,

ACPD
13, 1455–1488, 2013

Törő, N., Moerman, M., Henzing, B., de Leeuw, G., Brinkenberg, M., Kouvarakis, G. N., Bougiatioti, A., Mihalopoulos, N., O'Dowd, C., Ceburnis, D., Arneth, A., Svenningsson, B., Swietlicki, E., Tarozzi, L., Decesari, S., Facchini, M. C., Birmili, W., Sonntag, A., Wiedensohler, A., Boulon, J., Sellegri, K., Laj, P., Gysel, M., Bukowiecki, N., Weingartner, E., Wehrle, G., Laaksonen, A., Hamed, A., Joutsensaari, J., Petäjä, T., Kerminen, V.-M., and Kulmala, M.: EUCAARI ion spectrometer measurements at 12 European sites – analysis of new particle formation events, Atmos. Chem. Phys., 10, 7907–7927, doi:10.5194/acp-10-7907-2010, 2010.

McMurry, P. H., Fink, M., Sakurai, H., Stolzenburg, M. R., Mauldin, R. L., Smith, J., Eisele, F., Moore, K., Sjostedt, S., Tanner, D., Huey, L. G., Nowak, J. B., Edgerton, E., and Voisin, D.: A criterion for new particle formation in the sulfur-rich Atlanta atmosphere, J. Geophys. Res.-Atmos., 110, D22S02, doi:10.1029/2005JD005901, 2005.

Mirme, A., Tamm, A., Mordas, G., Vana, M., Uin, J., Mirme, S., Bernotas, T., Laakso, L., Hirsikko, A., and Kulmala, M.: A wide-range multi-channel Air Ion Spectrometer, Boreal Environ. Res., 12, 247–264, 2007.

Petäjä, T., Mauldin, III, R. L., Kosciuch, E., McGrath, J., Nieminen, T., Paasonen, P., Boy, M., Adamov, A., Kotiaho, T., and Kulmala, M.: Sulfuric acid and OH concentrations in a boreal forest site, Atmos. Chem. Phys., 9, 7435–7448, doi:10.5194/acp-9-7435-2009, 2009.

Pope, C. A. and Dockery, D. W.: Health effects of fine particulate air pollution: lines that connect, J. Air Waste Manage., 56, 709–742, 2006.

Ruuskanen, J., Tuch, T., Ten Brink, H., Peters, A., Khystov, A., Mirme, A., Kos, G. P. A., Brunekreef, B., Wichmann, H. E., Buzorius, G., Vallius, M., Kreyling, W. G., and Pekkanen, J.: Concentrations of ultrafine, fine and $PM_{2.5}$ particles in three European cities, Atmos. Environ., 35, 3729–3738, doi:10.1016/S1352-2310(00)00373-3, 2001.

Salma, I., Borsós, T., Weidinger, T., Aalto, P., Hussein, T., Dal Maso, M., and Kulmala, M.: Production, growth and properties of ultrafine atmospheric aerosol particles in an urban environment, Atmos. Chem. Phys., 11, 1339–1353, doi:10.5194/acp-11-1339-2011, 2011.

Sipilä, M., Berndt, T., Petäjä, T., Brus, D., Vanhanen, J., Stratmann, F., Patokoski, J., Mauldin III, R. L., Hyvärinen, A.-P., Lihavainen, H., and Kulmala, M.: The role of sulfuric acid in atmospheric nucleation, Science, 327, 1243–1246, doi:10.1126/science.1180315, 2010.

Sogacheva, L., Dal Maso, M., Kerminen, V.-M., and Kulmala, M.: Probability of nucleation events and aerosol particle concentration in different air mass types arriving at Hyytiala

ACPD
13, 1455–1488, 2013

southern Finland, based on back trajectories analysis, Boreal Environ. Res., 10, 479–491, 2005.
Stanier, C. O., Khlystov, A. Y., and Pandis, S. N.: Ambient aerosol size distributions and number concentrations measured during the Pittsburgh Air Quality Study (PAQS), Atmos. Environ., 38, 3275–3284, doi:10.1016/j.atmosenv.2004.03.020, 2004.
Twomey, A.: Pollution and the planetary albedo, Atmos. Environ., 8, 1251–1256, doi:10.1016/0004-6981(74)90004-3, 1974.
Twomey, S., Piepgrass, M., and Wolfe, T. L.: An assessment of the impact of pollution on global cloud albedo, Tellus B, 36, 356–366, doi:10.1111/j.1600-0889.1984.tb00254.x, 1984.
Twomey, S.: Aerosols, clouds and radiation, Atmos. Environ., 25A, 2435–2442, doi:10.1016/0960-1686(91)90159-5, 1991.
Wichmann, H. E. and Peters, A.: Epidemiological evidence of the effects of ultrafine particle exposure, Philos. T. R. Soc. Lond., 358, 2751–2769, doi:10.1098/rsta.2000.0682, 2000.
Woo, K. S., Chen, D. R., Pui, D. Y. H., and McMurry, P. H.: Measurements of Atlanta aerosol size distributions: observations of ultrafine particle events, Aerosol Sci. Tech., 34, 75–87, doi:10.1080/02786820120056, 2001.
Zhang R. Y., Suh, I., Zhao, J., Zhang, D., Fortner, E. C., Tie, X. X., Molina, L. T., and Molina, M. J.: Atmospheric new particle formation enhanced by organic acids, Science, 304, 1487–1489, doi:10.1126/science.1095139, 2004.

ACPD
13, 1455–1488, 2013

Table 1. Instruments used in this study.

Measurements	Instruments
Aerosol particles 6–800 nm	DMPS (University of Helsinki)
Air ions 0.8–42 nm	AIS (Airel Ltd., Estonia)
$PM_{2.5}$	TEI SHARP-5030
O_3	TEI 49i
SO_2	TEI 43i
Metrological parameters (air temperature, global radiation, wind, relative humidity)	CAMPBELL CR3000-TD

ACPD
13, 1455–1488, 2013

Table 2. Aerosol population statistics.

	Mean	5-perc.	25-perc.	Median	75-perc.	95-perc.
Total N [cm^{-3}]	**23 300**	9300	14600	**20 000**	26 400	38 700
Ion clusters [cm^{-3}]	**840**	240	600	**770**	970	1450
Nucl. mode [cm^{-3}]	**6700**	960	2100	**3500**	6000	14 300
Aitken mode [cm^{-3}]	**9500**	3700	6100	**8500**	11 500	18 700
Accu. mode [cm^{-3}]	**7100**	2500	4700	**6600**	9100	12 600
$PM_{2.5}$ [$\mu g\,m^{-3}$]	**90**	24	47	**79**	116	194
CS [$10^{-2}\,s^{-1}$]	**5.4**	1.7	3.0	**4.1**	5.6	7.7

ACPD
13, 1455–1488, 2013

Table 3. Event statistics.

	Event days	Non-event days	Undefined/no data
Nov (18–30)	**1**	5	8
Dec	**4**	23	4
Jan	**7**	13	11
Feb	**7**	12	10
Mar	**7**	12	16
TOTAL	**26**	65	45

ACPD
13, 1455–1488, 2013

Table 4. Event characteristics.

	Mean	5-perc.	25-perc.	Median	75-perc.	95-perc.
J_6 [$cm^{-3}\,s^{-1}$] (observed)	**1.1**	0.25	0.5	**0.8**	1.2	3.5
J_2 [$cm^{-3}\,s^{-1}$] (calculated)	**33.2**	2.6	14.8	**23.9**	56.8	75.6
GR 6–30 nm (DMPS) [$nm\,h^{-1}$]	**8.5**	4.5	6.1	**6.9**	10.9	15.4
GR 3–7 nm (AIS) [$nm\,h^{-1}$]	**6.3**	2.4	4.5	**5.9**	7.9	11.8
GR 7–30 nm (AIS) [$nm\,h^{-1}$]	**8.0**	3.5	5.2	**6.7**	8.2	16.0
CS [$10^{-2}\,s^{-1}$]	**2.4**	0.9	2.0	**2.5**	3.1	3.8
Q [$10^{6}\,cm^{-3}\,s^{-1}$]	**3.8**	1.0	2.2	**3.0**	5.5	7.5

GR = growth rate.
Q = source of condensable vapors.

ACPD
13, 1455–1488, 2013

Table 5. Aerosol numbers in Nanjing, Shanghai, and around the world.

	10 nm–100 nm	100 nm–500 nm	
Shanghai, CN	28 511	1676	Gao et al. (2009)
Nanjing, CN	13 000	6200	This work
Alkmaar, NL	18 300	2120	Ruuskanen et al. (2001)
Erfurt, DE	17 700	2270	Wichmann and Peters (2000)
Helsinki, FI	16 200	973	Ruuskanen et al. (2001)
Pittsburgh, US	14 300	2170	Stanier et al. (2004)
Atlanta, US	21 400	n/a	Woo et al. (2001)

ACPD
13, 1455–1488, 2013

Fig. 1. Location of the station within East China and the YRD.

ACPD
13, 1455–1488, 2013

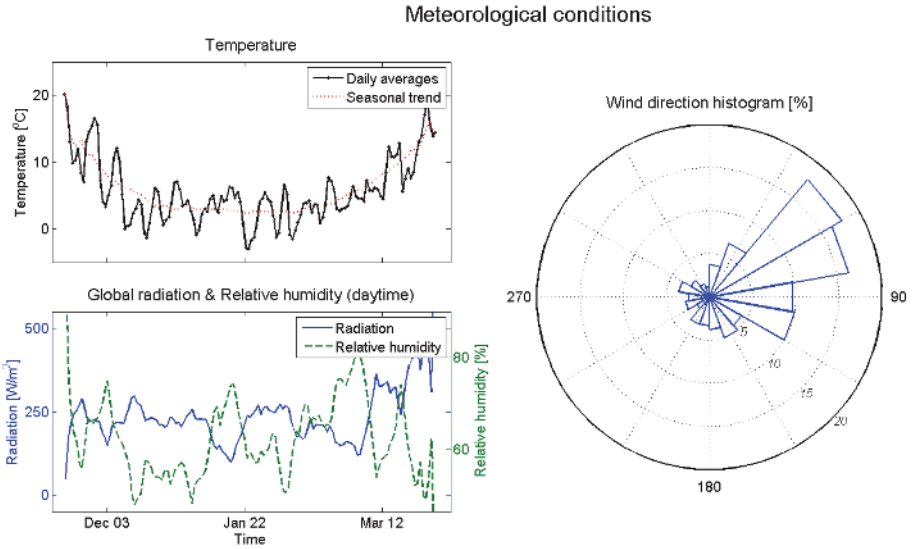

Fig. 2. Meteorological conditions during the measurement period 18 November–31 March.

ACPD
13, 1455–1488, 2013

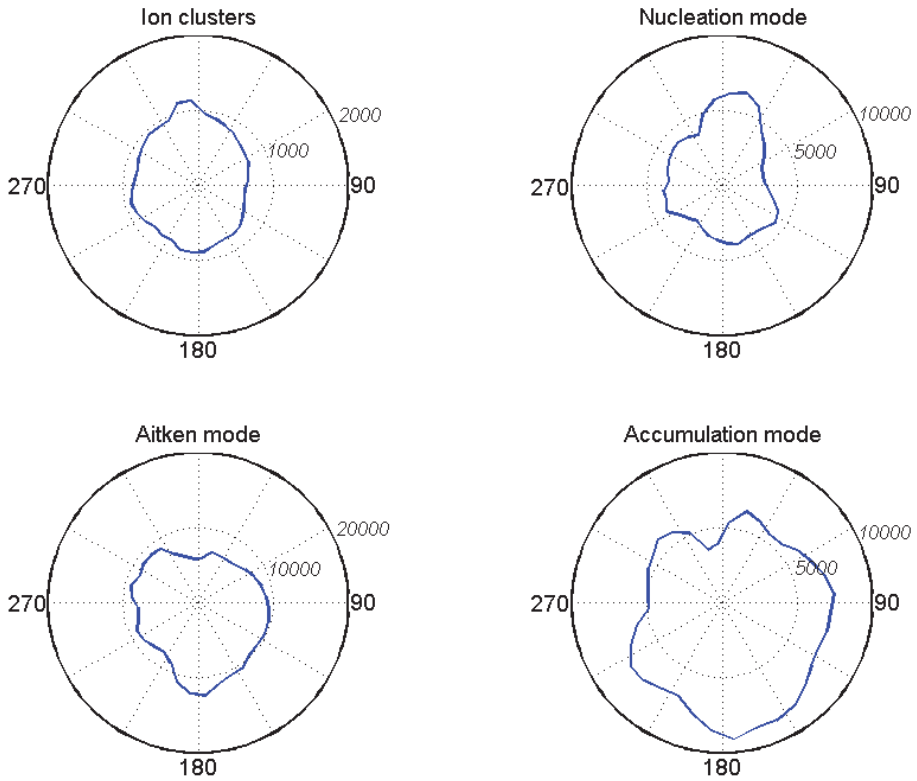

Fig. 3. Air ion and aerosol mode concentrations as a function of wind direction. Ion clusters: < 2 nm, nucleation mode: 6–25 nm, Aitken mode: 25–90 nm, accumulation mode: 90–800 nm.

ACPD
13, 1455–1488, 2013

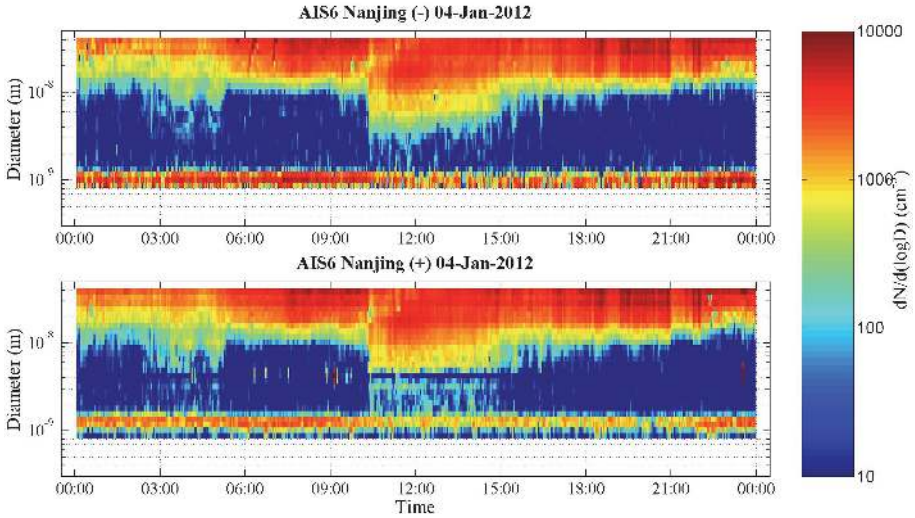

Fig. 4. Typical nucleation event with typical gap between cluster band and growth "banana".

ACPD
13, 1455–1488, 2013

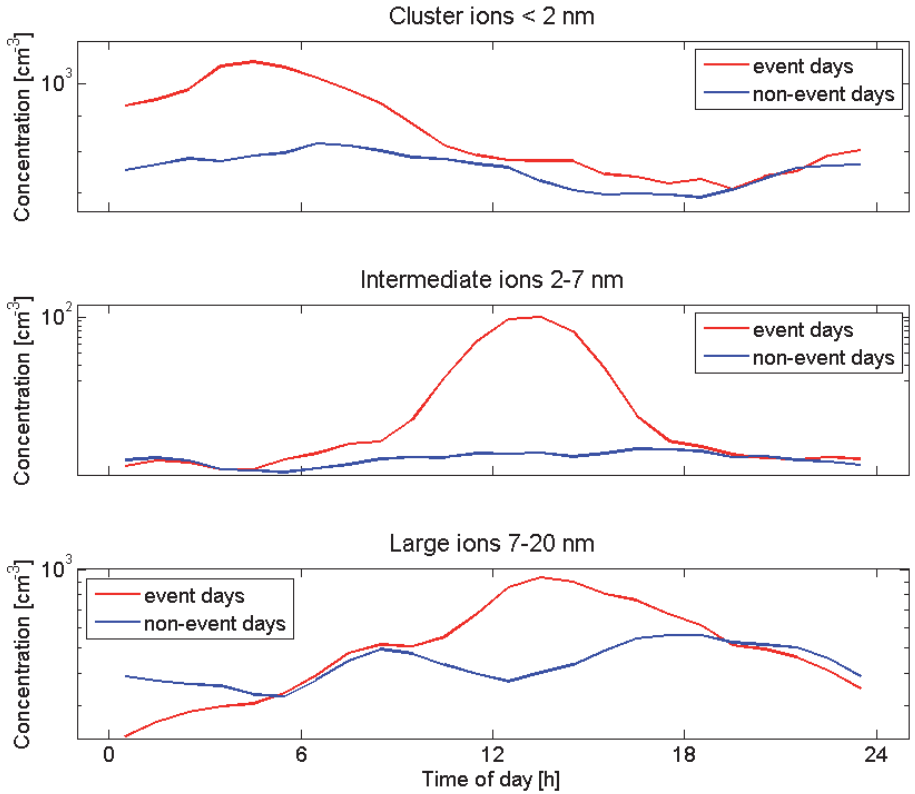

Fig. 5. Median daily cycles for different ion sizes, separated for days with and without new particle formation (event/non-event days).

ACPD
13, 1455–1488, 2013

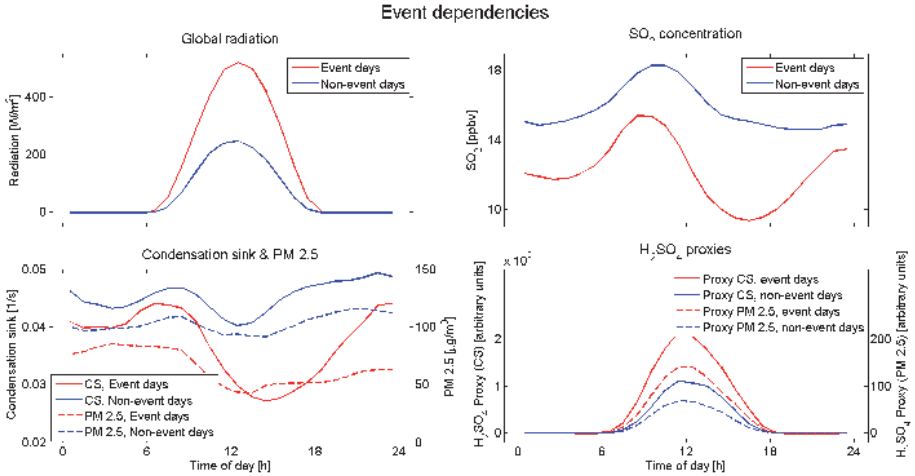

Fig. 6. Daily cycles of a number of relevant parameters for days with and without new particle formation.

ACPD
13, 1455–1488, 2013

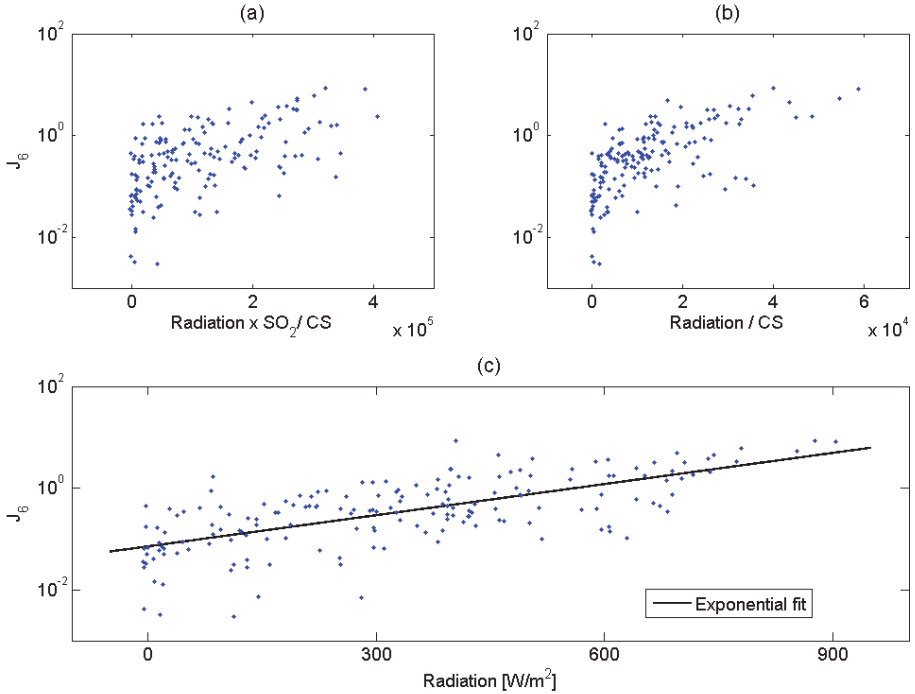

Fig. 7. Correlation between the observed particle formation rate J_6 and various parameters. For these plots, hourly averages of J_6 and the respective parameters where evaluated during new particle formation events.

ACPD
13, 1455–1488, 2013

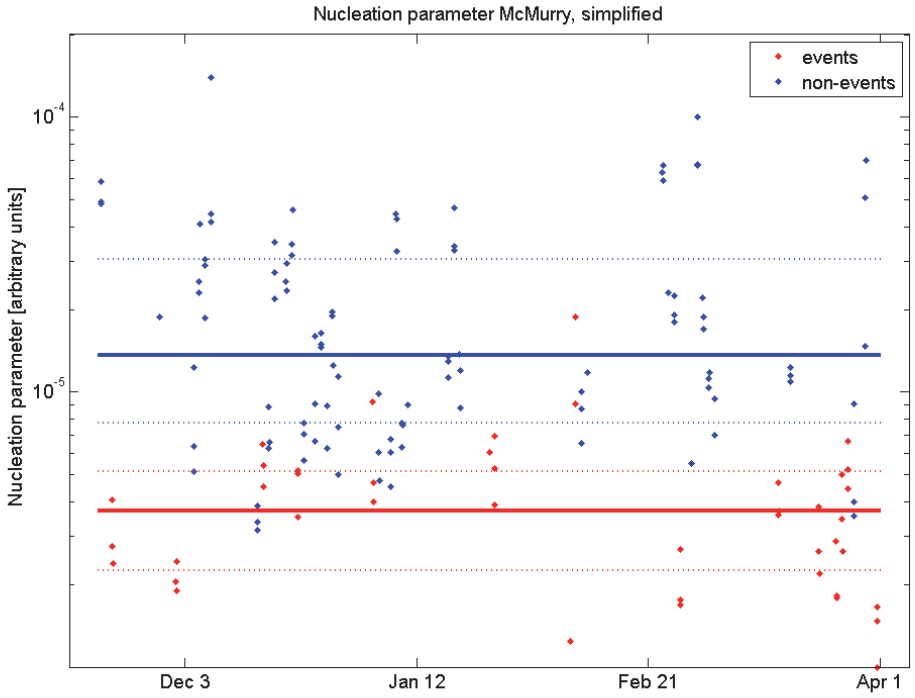

Fig. 8. Evaluation of a simplified nucleation parameter based on McMurry et al. (2005) with respective median values (full lines) and quartiles (dotted lines).

ACPD
13, 1455–1488, 2013

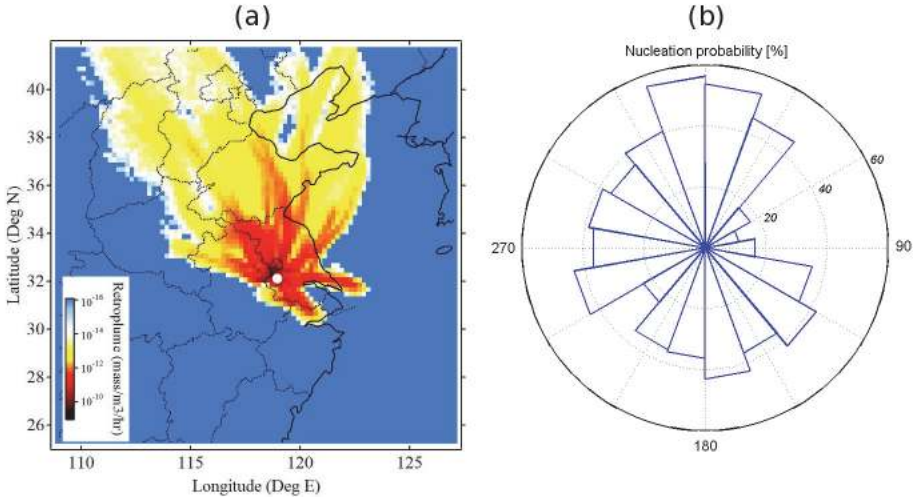

Fig. 9. (a) Retroplume for event days in a map of eastern China. The measurement site is marked by a dot. (b) Observed nucleation probability at the site as a function of the direction of the incoming air mass.

ACPD
13, 1455–1488, 2013